Array of Accelerometers as a Dynamic Vibro-Tactile Sensing for Assessing the Slipping Noise

Yerkebulan Massalim, Zhanat Kappassov

Array of Accelerometers as a Dynamic Vibro-Tactile Sensing for Assessing the Slipping Noise

Yerkebulan Massalim *Student Member, IEEE*, Zhanat Kappassov, *Member, IEEE*

***Abstract*— Through vibrations people can assess both slippage of the directly grasped object and sliding of an external agent over the surface of the grasped immovable object. In robotic hands, with less advanced tactile sensing, the slippage and sliding events can be hard to distinguish. This paper shows how vibro-tactile sensing array can help to distinguish object/world sliding and sensor/object slippage events based on cross-correlation, which computes similarity in sensor readings of tactile array cells. The proposed vibro-tactile system consists of two accelerometers. Experiments with different surfaces are conducted to test the system and the proposed algorithm.**

I. Introduction

There is evidence that people can detect and assess motions of a grasped object through vibrations [1]. When the surface moves, a human hand experiences mechanical vibrations. This phenomenon is known as a structure-borne sound [2]. Using an accelerometer and a recoil actuator [3], experiments in human tactile perception revealed that simulations of only the structure-borne sound cause haptic illusion of a moving surface.

In this paper, we present a vibro-tactile sensor with an array of high-bandwidth accelerometers that can measure the structure-borne sound. Using this array, we compute coherence of a group of measurements of the tactile array. Thus, we are able to find out whether these measurements belong to a single waveform or to a group of incoherent ones.

Development of vibro-tactile sensors has been motivated, but not limited to, by a need for stable grasping using robot hands and grippers [4], [5]. The absence of structure-borne sound (vibrations) indicates that no slippage is registered. Method of achieving stable grasping via detecting vibrations has long been implemented in hand prosthetic devices [6]. Sensor/object slippage can be recognized in time domain by registering the high-pass filtered tactile signals from capacitive sensors, e.g. Pressure Profile Systems (PPS) sensors [7]. Also, such tactile signals can be detected from a spectral power in the frequency domain using Fast Fourier transformations (FFT) as shown in [8]. Similar registration but in time-frequency domain via discrete wavelet transformations (DWT) is given in [9]. The latter approaches can be optimized to reduce the computational cost by extracting principal components (PCA) and classifying, e.g. $k-$nearest neighbors ($k-$NN), the extracted components of signals transformed with short time Fourier Transformation (STFT) [11]. Other approaches use less direct techniques, such as image processing tools and an array of piezoelectric sensors as demonstrated in [12]. The authors can predict slippage by comparing a number of shifted contact points with a number of non-shifted contact ones. Vision cameras featured with a higher sampling rate are capable of tracking displacements of contact points to detect slippage events [13]. In addition, recently emerged event-based cameras are capable of detecting changes in images immediately [14]. Similar approaches apply computer vision techniques to clarify the output of tactile arrays by considering them as grayscale images. On the other hand, vibrations recorded via accelerometers warn about both a first contact with the environment and slippage [7]. A more direct way of slippage detection includes measurements of tangential forces [16] and Coulomb friction cone models

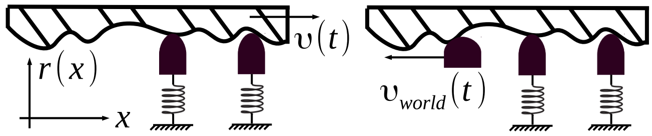

Fig. 1: Raw model of the vibrations generated by (a): a moving surface in contact with sensors (b): a moving world in contact with a surface

TABLE I: Approaches for the slippage detection based on tactile information

Sensors	Transduction	Methods
Microphone [6]	Acoustic	High-pass filter
PPS sensors [7]	Capacitive	High-pass filter
Polyvinylidene fluoride [9]	Piezoelectric	DWT
Capacitive sensors [8], [10]	Capacitive	FFT, spectral power, object/surface detection
Polyvinylidene fluoride [11]	Piezoelectric	STFT, PCA, $k-$NN
Accelerometer [7]	Acoustic	Filter, contact detection
Piezoelectric (16x16) [12]	Piezoelectric	Computer vision techniques
TacTip [13]	Optical	Image processing
Event-based camera [14]	Optical	Image processing
ATi nano 17 [15]	Strain gauges	Force sensors, Coulomb forces

This work was partially supported by the Ministry of Education and Science of the Republic of Kazakhstan and Nazarbayev University grants.

authors are with the Dept. of Robotics and Mechatronics, Nazarbayev University, 53 Kabanbay Batyr Ave, Z05H0P9 Astana, Kazakhstan. Email: {yerkebulan.massalim, zhkappassov}@nu.edu.kz.
Corresponding author: Z. Kappassov.

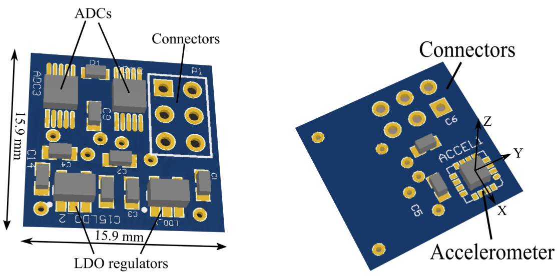

(a) (b)

Fig. 2: Sensor module printed circuit board: (a) top (b) bottom views.

[15]. Combination of friction force signals and vibro-tactile signals can be used to achieve a stable robot non-prehensile manipulation [17]. Table I lists the aforementioned slippage detection techniques.

Among the reviewed literature, however, there is no much work dealing with robot dynamic tactile sensors capable of tackling the problem of distinguishing object/sensor (Fig. 1a) slippage from object/world (Fig. 1b) sliding [18]. In case of object/sensor slippage, velocity $v(t)$ is not zero, whereas $v(t)$ is zero in object/world sliding. For this purpose, in our proposed vibro-tactile sensing array we use signal conditioning electronics that deliver a synchronized stream of data registered on all sensing modules. These sensing modules are isolated from each other by air. Presumably, our approach can be integrated into autonomous dexterous manipulation routines for assuring a stable grasp with multiple points of contact as described in [19].

Our vibro-tactile sensor design (Fig. 2) is presented in the next section and followed by the description of the method for slip assessment. The developed setup (Fig. 6) of the sensing array and experimental results with three different surface profiles are described in Section IV. Section V concludes the paper and discusses future works.

II. Vibro-tactile sensing module

The design of human fingertip and the fact that it can detect structure-borne sounds with frequency of up to 1 kHz provides a general concept of slippage detection systems [20]. In our design, sensing modules measure vibrations at contact points simultaneously and quickly without interfering each other. Generally, we can specify the desired properties of the vibro-tactile sensing module as follows:

1) in order to detect vibrations during slippage, the sensing module should have appropriate physical bandwidth to detect the structure-borne sounds;

2) a signal conditioning circuit should have an appropriate data acquisition bandwidth;

3) sensor signals should be sampled synchronously;

4) be small enough to accommodate all electronic components;

5) be mechanically isolated from each other to avoid unwanted parasitic vibrations;

6) be easily manufactured and replicated by a person with basic technical skills;

7) be cost effective;

8) be reliable and maintainable.

A. Accelerometers

Vibration sensor module consists of one high-bandwidth-three-axes accelerometer with analog output and a pair of Analog Devices AD7685 which sample accelerometer measurements along x and y axes (Fig. 2).

The accelerometer has physical bandwidth of more than 1 kHz. Such bandwidth allows to capture vibrations resulting from movements during slips in commonly accepted range of frequencies [20]. Also, an ordinary first-order filter (with time constant $\tau_{RC} = 1\mu s$) is used as anti-aliasing filter.

AD7685 is a tiny 16-bit analog-to-digital converter (ADC) with a suitable size to build up an array of sensors with small overall dimensions. It can provide up to 220 kHz sampling rate. Another important advantage of the chip is supporting cascaded connections while preventing the sampling rate to decline and the number of control pints to increase. Using several pins of a microcontroller unit, it is possible to acquire synchronized data from up to eight ADC chips at the maximum sampling rate for every chip. Therefore, we can connect multiple accelerometers in a cascaded manner.

We use two vibro-tactile sensing modules to construct the vibro-tactile sensing array. Therefore, we connect four ADCs: two chips per each module.

B. ARM microcontroller based control unit

The main function of ARM microcontroller unit (Fig. 4) is to synchronously condition signals from ADCs at a constant frequency and deliver them to a host computer via a communication protocol, e.g. USB. The main element of this unit is STM32F3 ARM microcontroller with 72 MHz clock. The speed and computational power of the microcontroller provide enough potential to achieve four channel 32 kHz sampling rate for aforementioned ADC. Thus, 8 kHz of sampling rate for every channel is enough to sample each accelerometer data since it has maximum bandwidth of 1.5 kHz. Fig. 3 summarizes the structure of the sensing array and control unit in a block diagram.

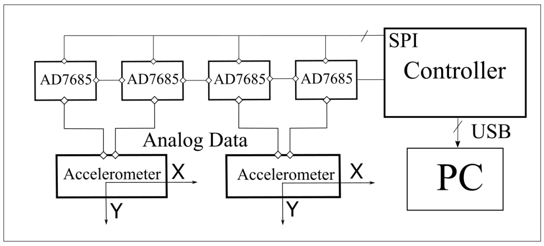

Fig. 3: Block diagram of the vibro-tactile array

III. Slippage vibration assessment algorithm

Using the sensing modules described above, we can infer the rugosity function (surface profile) $r(x)$ of the surface given in Fig. 1a. The values of the $r(x)$ as a function of the surface displacement $x(t)$ at velocity $v(t)$ results

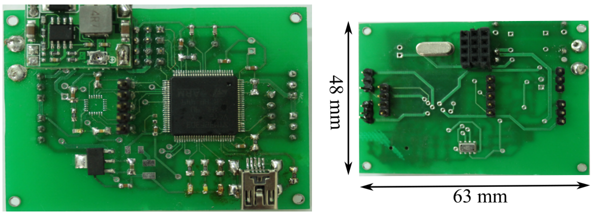

(a) (b)

Fig. 4: Custom ARM microcontroller board: (a) Top side, (b) Bottom side

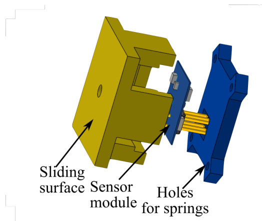

Fig. 5: Vibro-tactile sensing module assembly

in a vibration signal that is proportional to the derivative $r'(x(t))v(t)$.

The main basis of the proposed slippage assessment algorithm lies on investigating $r'(x(t))v(t)$ for two different cases: object/sensor slippage (Fig. 1a) and object/world sliding (Fig. 1b). We assume that vibrations propagate and reach sensors at infinitely small amount of time, so the phase difference does not occur in readings of these sensors. This assumption is valid as long as

$$\frac{1}{F_s} >> max(t_{pd}) \tag{1}$$

where t_{pd} is the time lag in sensor readings due to the vibration propagation speed, F_s is the sampling rate of 8 kHz. As it is described in Section IV-A, the distance between sensors is 10 cm. Assuming that speed of propagation of structure-borne sound in object is more than 2000 m/s, t_{pd} is less than 50 μs. Therefore, it can be assumed that a particular structure-borne sound wave causes similar accelerations in all cells of a tactile sensing array.

In the first case, when the surface slips over sensors, each sensing cell reads local sensor-motion vibrations. In this case signals are not correlated.

In the second case, when the surface vibrates due to environmental impact, the same forces will affect sensor readings. Hence, waves of vibrations reach all sensing cells of a tactile array simultaneously, and, therefore, sampled signals are correlated.

A. Correlation estimation

Let's define R_i as readings of an ith accelerometer that captures vibrations $r'(x(t))v(t)$ due to surface roughness. Then the correlation of two sensor readings (R_a, R_b) is defined as the normalized cross-correlation function of the signals:

$$C_{a,b} = \frac{(R_a - \overline{R_a})^T * (R_b - \overline{R_b})}{\sqrt{{R_a^2}^T * R_b^2}} \tag{2}$$

where R_a and $R_b \in \mathcal{R}^N$, N is window size of the first and second accelerometer readings, respectively. Since it is not necessary to estimate delayed correlation, it is neglected.

$C_{a,b}$ value lies in the range of [0, 1]. When $C_{a,b} \approx 1$, R_a and R_b are correlated. Otherwise, when $C_{a,b}$ is close to zero, sensor readings are not correlated, i.e. different from each other.

Therefore, when a sliding motion occurs between the environment and the grasped object, signals are perfectly correlated and C_a, b is equal to one. In contrast, when the object slips over sensors, structure-borne sound is generated at each contact and it leads $C_{a,b}$ to be close to zero.

Thus, $C_{a,b}$ correlation feature provides similarity degree of sensor readings. It depends on whether slippage or sliding occurs.

In real-time robot control applications, it is desirable to optimize computational costs. Therefore, we should eliminate redundancy during the normalized cross correlation computation. It is necessary to update its value in every iteration, but past iterations can be used to optimize computational efforts.

As proposed in [21], we exploit modified version of sum tables to reach the minimum computation time. We consider W size $R_i(u)$ real-time FIFO buffer and assume that phase difference does not exist between sensor data. Therefore, we can compute the following modified digital representations $s_a(u)$ and $s_b(u)$ of R_a and R_b, respectively

$$s_a(u) = \begin{cases} s_a(u-1) + R_a^2(u) - R_a^2(u-W), & u\text{>W} \\ s_a(u-1) + R_a^2(u), & u\text{>0} \\ 0, & u\text{= 0} \end{cases} \tag{3}$$

$$s_b(u) = \begin{cases} s_b(u-1) + R_b^2(u) - R_b^2(u-W), & u\text{> W} \\ s_b(u-1) + R_b^2(u), & u\text{> 0} \\ 0, & u\text{= 0} \end{cases} \tag{4}$$

Thus, their cross-correlation

$$s_{a,b}(u) = \begin{cases} s_{a,b}(u-1) + R_a(u)R_b(u), & u\text{> 0} \\ 0, & u\text{= 0} \end{cases} \tag{5}$$

Finally, the normalized cross-correlation (NCC)

$$C_{a,b}(u) = \frac{s_{a,b}(u)}{\sqrt{s_a(u)s_a(u)}} \tag{6}$$

IV. Experiments

The proposed sensing array is validated in a series of experiments by applying the latter equation (6). In the following section, we describe our setup, experimental scenario, and results.

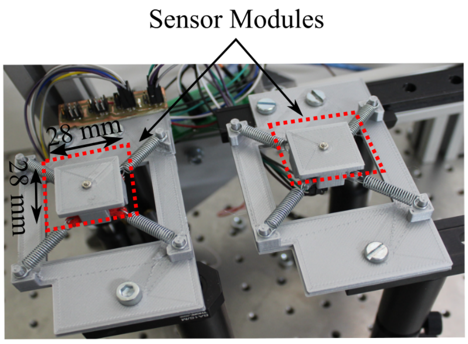

Fig. 6: General view of the setup

A. Setup

Each vibro-tactile sensing module (Fig. 5) is held by four series elastic elements (helical extension springs). They are attached to fastening tabs at corners of a module from one side and fixed to a rigid structure from the other side. The rigid structure is built on an optical breadboard using mounting clamps and platforms (Fig. 6).

The distance between the modules is 10 cm in horizontal plane. They are aligned in vertical plane. The ARM microcontroller unit is attached onto one of the mounting platforms.

B. Experimental scenario

During the experiment, different kinds of surface profiles are used to ensure that the algorithm performance does not depend on a surface profile type. Fig. 7 illustrates three objects with different surface profiles. The first object is aluminum profile, the second object is a textile, attached onto a rigid plastic piece and the third one is a wooden stick.

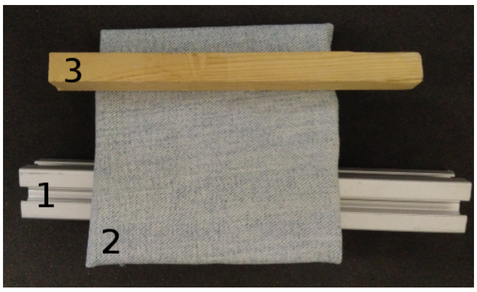

Fig. 7: Objects with different surface profiles:
1 - aluminum, 2 - textile, 3 - wood.

In order to imitate real conditions of object/sensor slippage (Fig. 1a) as close as possible, an operator moves objects as shown in Fig. 8a. The speed of the slippage is also varied.

Then, in order to re-create the situation when the environment slides over an immovable object (Fig. 1b), an operator slides an object over the same three objects, which are immovable (Fig. 8b).

C. Results

The recorded signals from the vibro-tactile array are processed in MATLAB to distinguish world-object sliding from object-sensor slippage. Since, the sensing modules of the array deliver data simultaneously, the problem of phase shift does not occur. We also apply band-stop filter (65 Hz) to attenuate the effect of the springs that hold the sensing modules.

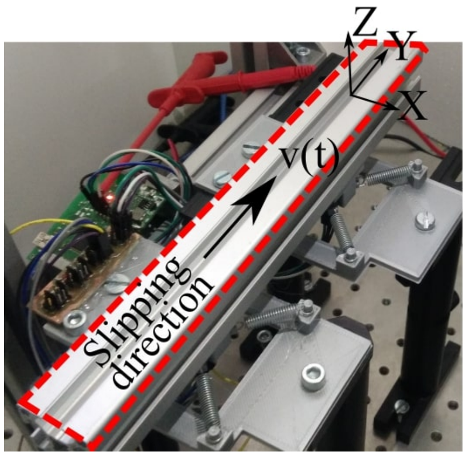

(a)

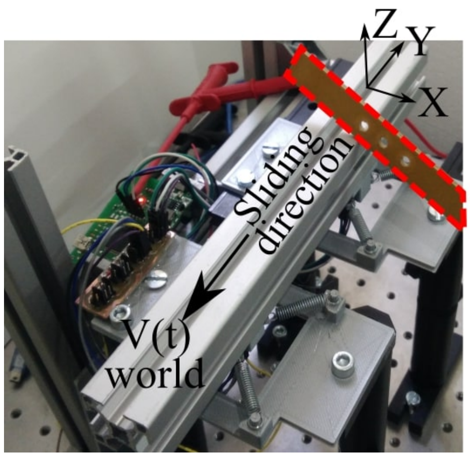

(b)

Fig. 8: Experimental scenario: (a) object/sensor slippage, (b) object/environment sliding

Fig. 9 shows the raw acceleration data of two sensing modules and NCC, recorded for the three objects described above. The figure shows accelerations that occur along x-axis. In the illustrated results, the time window for obtaining NCC is equal to 2000 samples (0.25 s), i.e. $W = 2000$. NCC and signals shown in Fig. 9 a, b, and c correspond to objects 1, 2, 3 in Fig. 7, respectively.

The shaded sides of Fig. 9 a, b, c correspond to the case when an object slips over sensing array. Since the rugosity function is different at each sensing module, NCC is close to zero and does not reach half of its maximum. On the other hand, in case when the object is immovable and another object slides over it, NCC tends to its maximum (non-shaded side) since the rugosity function is the same at each sensing module. So far, we observe that cross-correlation is higher in case when the world slides over the immovable object than in case when the object slips over the vibro-tactile sensing array.

By changing the size of time-window for obtaining NCC,

TABLE II: Mean and standard deviation of NCC

	Aluminum			*Textile*			*Wood*		
	$W = 3000$	$W = 1500$	$W = 500$	$W = 3000$	$W = 1500$	$W = 500$	$W = 3000$	$W = 1500$	$W = 500$
Slippage									
σ	0.067	0.119	0.187	0.060	0.090	0.170	0.083	0.114	0.192
mean	-0.040	-0.036	-0.037	-0.015	-0.003	0.012	0.109	0.093	0.065
Sliding									
σ	0.105	0.165	0.235	0.072	0.098	0.148	0.106	0.119	0.150
mean	0.414	0.377	0.331	0.620	0.617	0.607	0.668	0.670	0.685

we observe that the standard deviation, σ is inversely proportional to W. For real-time applications, it leads to the trade-off between the robustness and response time. We also observe that the difference of NCC between slippage and sliding conditions is larger for a textile than for an aluminum bar and wooden stick. Therefore, these two conditions are more distinguishable for the textile than for the rest of the objects. These observations are summarized in Table II.

V. Conclusions

In this work, we present the design and implementation of a vibro-tactile sensing array which allows detection of slippage and sliding events during physical interactions. The working principle is based on measuring the acceleration caused by surface roughness. We show that classification of the object/sensor slippage and object/world sliding can be achieved using this sensing array. In order to demonstrate the efficacy, we benchmark the proposed approach in experiments with three different objects.

As future work, we envision to embed the sensing array into a robot gripper and implement the proposed algorithm directly in a microcontroller unit.

[22] [23] [24] [25]

Acknowledgements

The authors are thankful to Vincent HAYWARD for discussions on human perception aspects, especially haptics. We would like to thank Almas SHINTEMIROV and Atakan VAROL for sharing lab facilities and discussions on technical aspects of implementation.

References

[1] H.-Y. Yao and V. Hayward, "An experiment on length perception with a virtual rolling stone," in *in: Proceedings of Eurohaptics*, 2006, pp. 325–330.

[2] R. D. Howe and M. R. Cutkosky, "Sensing skin acceleration for slip and texture perception," in *International Conference on Robotics and Automation(ICRA)*, May 1989, pp. 145–150 vol.1, doi: 10.1109/ROBOT.1989.99981

[3] H. Yao and V. Hayward, "Design and analysis of a recoil-type vibrotactile transducer," *The Journal of the Acoustical Society of America*, vol. 128, no. 2, pp. 619–627, August 2010, doi: 10.1121/1.3458852

[4] Z. Kappassov, J.-A. Corrales, and V. Perdereau, "Tactile sensing in dexterous robot hands," *Robotics and Autonomous Systems*, pp. 195–220, July 2015, doi: 10.1016/j.robot.2015.07.015

[5] S. Luo, W. Mou, K. Althoefer, and H. Liu, "iclap: shape recognition by combining proprioception and touch sensing," *Autonomous Robots*, pp. 1–12, 2018, doi: 10.1007/s10514-018-9777-7

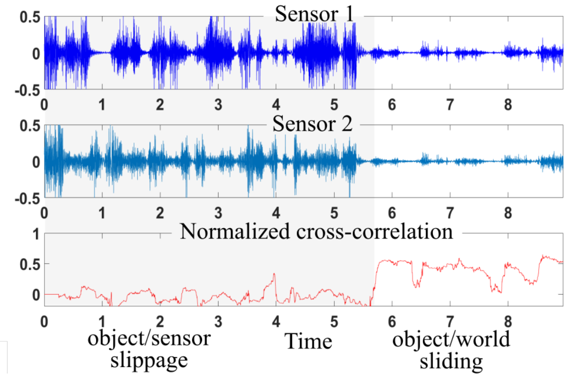

(a)

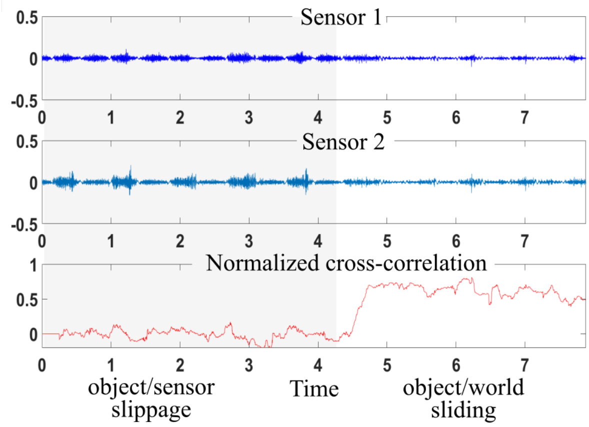

(b)

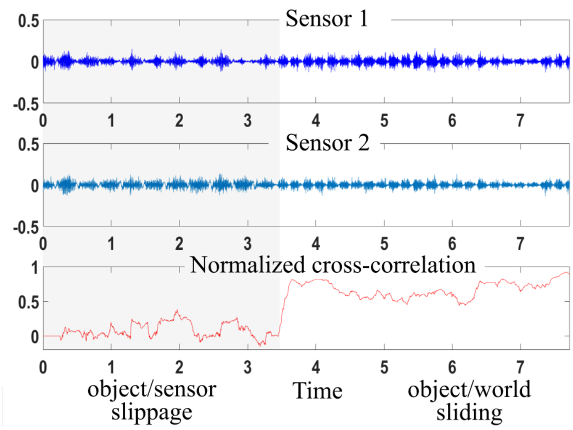

(c)

Fig. 9: Cross-correlation function results over 3 different surface profiles: (a) Aluminum, (b) Textile, (c) Wood

[6] P. J. Kyberd, M. Evans, and S. te Winkel, "An intelligent anthropomorphic hand, with automatic grasp," *Robotica*, vol. 16, pp. 531–536, September 1998.

[7] J. Romano, K. Hsiao, G. Niemeyer, S. Chitta, and K. Kuchenbecker, "Human-inspired robotic grasp control with tactile sensing," *Robotics, IEEE Transactions on*, no. 6, pp. 1067–1079, Dec 2011, doi: 10.1109/TRO.2011.2162271

[8] M. R. Cutkosky and J. Ulmen, "Dynamic tactile sensing," in *The Human Hand as an Inspiration for Robot Hand Development*. Springer, 2014, pp. 389–403.

[9] S. Teshigawara, T. Tsutsumi, S. Shimizu, Y. Suzuki, A. Ming, M. Ishikawa, and M. Shimojo, "Highly sensitive sensor for detection of initial slip and its application in a multi-fingered robot hand," in *International Conference on Robotics and Automation(ICRA)*, May 2011, pp. 1097–1102, doi: 10.1109/ICRA.2011.5979750

[10] X. A. Wu, N. Burkhard, B. Heyneman, R. Valen, and M. Cutkosky, "Contact event detection for robotic oil drilling," in *IEEE International Conference on Robotics and Automation(ICRA)*, May 2014, pp. 2255–2261.

[11] D. Göger, N. Gorges, and H. Worn, "Tactile sensing for an anthropomorphic robotic hand: Hardware and signal processing," in *International Conference on Robotics and Automation(ICRA)*, May 2009, pp. 895–901, doi: 10.1109/ROBOT.2009.5152650

[12] V. A. Ho, T. Nagatani, A. Noda, and S. Hirai, "What can be inferred from a tactile arrayed sensor in autonomous in-hand manipulation?" in *International Conference on Automation Science and Engineering (CASE)*, Aug 2012, pp. 461–468.

[13] J. W. James, N. Pestell, and N. F. Lepora, "Slip detection with a biomimetic tactile sensor," *IEEE Robotics and Automation Letters*, vol. 3, no. 4, pp. 3340–3346, Oct 2018, doi: 10.1109/LRA.2018.2852797

[14] A. Rigi, F. Baghaei Naeini, D. Makris, and Y. Zweiri, "A novel event-based incipient slip detection using dynamic active-pixel vision sensor (davis)," *Sensors*, vol. 18, no. 2, January 2018, doi: 10.3390/s18020333

[15] X. Song, H. Liu, K. Althoefer, T. Nanayakkara, and L. Seneviratne, "Efficient break-away friction ratio and slip prediction based on haptic surface exploration," *IEEE Transactions on Robotics*, vol. 30, no. 1, pp. 203–219, Feb 2014, doi: 10.1109/TRO.2013.2279630

[16] V. A. Ho, D. V. Dao, S. Sugiyama, and S. Hirai, "Development and analysis of a sliding tactile soft fingertip embedded with a microforce/moment sensor," *IEEE Transactions on Robotics*, vol. 27, no. 3, pp. 411–424, June 2011, doi: 10.1109/TRO.2010.2103470

[17] M. Meier, G. Walck, R. Haschke, and H. J. Ritter, "Distinguishing sliding from slipping during object pushing," in *International Conference on Intelligent Robots and Systems(IROS)*, Oct 2016, pp. 5579–5584, doi: 10.1109/IROS.2016.7759820

[18] B. Heyneman and M. R. Cutkosky, "Slip classification for dynamic tactile array sensors," *The International Journal of Robotics Research*, vol. 35, no. 4, pp. 404–421, March 2015, doi: 10.1177/0278364914564703

[19] N. Sommer and A. Billard, "Multi-contact haptic exploration and grasping with tactile sensors," *Robotics and Autonomous Systems*, vol. 85, pp. 48–61, Nov. 2016, doi: 10.1016/j.robot.2016.08.007

[20] R. S. Johansson and J. R. Flanagan, "Coding and use of tactile signals from the fingertips in object manipulation tasks," *Nature Reviews Neuroscience*, vol. 10, no. 5, pp. 345–359, May 2009, doi: 10.1038/nrn2621

[21] J. Luo and E. E. Konofagou, "A fast normalized cross-correlation calculation method for motion estimation," *IEEE Transactions on Ultrasonics, Ferroelectrics, and Frequency Control*, vol. 57, no. 6, pp. 1347–1357, June 2010, doi: 10.1109/TUFFC.2010.1554

[22] Y. Massalim and Z. Kappassov, "Array of accelerometers as a dy-

namic vibro-tactile sensing for assessing the slipping noise," in *2019 IEEE/SICE International Symposium on System Integration (SII)*. IEEE, 2019, pp. 438–443.

[23] A. Khamitov, Y. Massalim, and A. Ruderman, "Simultaneous selective harmonic elimination and total harmonic distortion minimization for a single-phase two-level inverter," in *2017 International Conference on Optimization of Electrical and Electronic Equipment (OPTIM) & 2017 Intl Aegean Conference on Electrical Machines and Power Electronics (ACEMP)*. IEEE, 2017, pp. 735–740.

[24] S. P. Chinchali, S. C. Livingston, M. Chen, and M. Pavone, "Multi-objective optimal control for proactive decision making with temporal logic models," *The International Journal of Robotics Research*, vol. 0, no. 0, p. 0278364919868290, 0.

[25] A. Mazhitov, A. Adilkhanov, Y. Massalim, Z. Kappassov, and H. A. Varol, "Deformable object recognition using proprioceptive and exteroceptive tactile sensing," in *2019 IEEE/SICE International Symposium on System Integration (SII)*. IEEE, 2019, pp. 734–739.